Application of Seven-Level Neural Space Vector PWM in DVC Control System of a DFIG for Wind Turbine

Habib Benbouhenni
* Laboratoire d'Automatique et d'Analyse des Systèmes (LAAS), Departement de Génie Electrique, Ecole Nationale Polytechnique d'Oran Maurice Audin, Oran, Algeria.
(habib0264@gmail.com)
‡ Corresponding Author; Habib Benbouhenni, BP: 50B Ouled Fares Chlef Algeria, Tel: +213663956329, habib0264@gmail.com

Received: 09.07.2019 Accepted:07.09.2019

Abstract- This paper presents the direct vector control (DVC) technique of doubly fed induction generator (DFIG) with the application of seven-level neural space vector pulse width modulation (7L-NSVPWM). The mathematical model of the DFIG has been described. The descriptions of the 7L-SVPWM technique and neural networks (NNs) have been presented. The DVC control scheme with 7L-NSVPWM technique has been described. The simulation results of the DVC control with 7L-NSVPWM strategy have been performed, and the results of these simulations are presented and discussed.
Keywords: DFIG, 7L-NSVPWM, 7L-SVPWM, NNs, DVC.

Nomenclature

L_r, L_s	Stator and rotor self-inductances.
L_m	Mutual inductance.
R_r, R_s	Stator and rotor resistances.
ψ_r, ψ_s	Rotor and Stator flux vectors.
I_s, I_r	Rotor and stator current vectors.
V_s, V_r	Rotor and stator voltage vectors.
P_s, Q_s	Active and reactive powers.

Subscripts

r, s	Rotor, stator.
d, q	Synchronous d-q axis.

1. Introduction

The main objective of this work is the studying of the direct vector control (DVC) with seven-level space vector pulse width modulation (DVC-7L-SVPWM) and DVC strategy with seven-level neural SVPWM (DVC-7L-NSVPWM) applied to the doubly fed induction generator (DFIG) therefore; our paper is organized as follows:

The first part is devoted to the a mathematical model of the DFIG, the model will simulate generator mode.

In the second part, we presente a mathematical model of the seven-level NPC inverter.

The third is devoted to the study of the technical modulation technique 7L-SVPWM and 7L-NSVPWM techniques. Finally, we presente a DVC control with 7L-SVPWM and 7L-NSVPWM techniques.

2. Modeling of the DFIG

The equations of fluxes and voltages for the DFIG stator and rotor in Park orientation structure are given by [1, 2]:

$$\begin{cases} V_{ds} = R_s I_{ds} + \frac{d}{dt}\Psi_{ds} - \omega_s \Psi_{qs} \\ V_{qs} = R_s I_{qs} + \frac{d}{dt}\Psi_{qs} + \omega_s \Psi_{ds} \\ V_{dr} = R_r I_{dr} + \frac{d}{dt}\Psi_{dr} - \omega_r \Psi_{qr} \\ V_{qr} = R_r I_{qr} + \frac{d}{dt}\Psi_{qr} + \omega_r \Psi_{dr} \end{cases} \tag{1}$$

The stator and rotor flux can be expressed as:

$$\begin{cases} \psi_{ds} = L_s I_{ds} + M I_{dr} \\ \psi_{qs} = L_s I_{qs} + M I_{qr} \\ \psi_{dr} = L_r I_{dr} + M I_{ds} \\ \psi_{qr} = L_r I_{qr} + M I_{qs} \end{cases} \tag{2}$$

The reactive and active powers can be written as:

$$\begin{cases} P_s = \dfrac{3}{2}(V_{ds}I_{ds} + V_{qs}I_{qs}) \\ Q_s = \dfrac{3}{2}(V_{qs}I_{ds} - V_{ds}I_{qs}) \end{cases} \tag{3}$$

The torque is given by:

$$T_{em} = \frac{3}{2} p \frac{M}{L_s}(\psi_{qs}I_{dr} - \psi_{ds}I_{qr}) \tag{4}$$

The electrical model of the DFIG is completed by the following mechanical equation :

$$T_{em} = T_r + J \cdot \frac{d\Omega}{dt} + f \cdot \Omega \tag{5}$$

Where :

Ids and Iqs are the stator currents.
ψdr and ψqr are the rotor fluxes.
ψds and ψqs are the stator fluxes.
Vdr, and Vqr are the rotor voltages.
Vqs and Vds are the stator voltages.
ωs : is the electrical pulsation of the stator .
Idr, and Iqr are the rotor currents.
p : is the number of pole pairs.
M : is the mutual inductance.
ωr : is the electrical pulsation of the rotor.
f : is the viscous friction coefficient.
Te : is the electromagnetic torque.
Ω : is the mechanical rotor speed.
J : is the inertia.
Tr : is the load torque.

3. Seven-level NPC inverter

Multilevel inverters (MIs) continue to receive more and more attention because of their low switching losses, high voltage operation capability, high efficiency and low output of electro magnetic interference [3]. The term MI starts with the three-level inverter introduced by Nabae et al (1981) [4]. Nowadays, MIs are becoming increasingly popular in power applications, as MIs have the ability to meet the increasing demand of power rating and power quality associated with lower electromagnetic interference and reduced harmonic distortion (THD). There are three main types of MIs: capacitor-clamped (flying capacitors), cascaded H-bridge and diode-clamped (neutral-clamped) inverter [5]. In this paper, we propose to use a seven-level neutral-point clamped inverter (NPC) to fed the rotor of the DFIG.

The seven-level NPC inverter consists of two pairs of series switches in parallel with six series capacitors where the anode of the upper diode is connected to the neutral of the capacitors and its cathode to the neutral of the upper pair of switches; the cathode of the lower diode is connected to the neutral of the capacitors and divides the main DC voltage into smaller voltages, which is shown in Fig. 1.

The voltage across the phase winding of the DFIG can attain one of the 7 levels 0, 1, 2, 3, 4, 5 or 6 depending upon the switching states of the inverters. The necessary conditions for the switching states for the 7 levels NPC are that the DC-link capacitors should not be shorted, and the output current should be continuous [6].

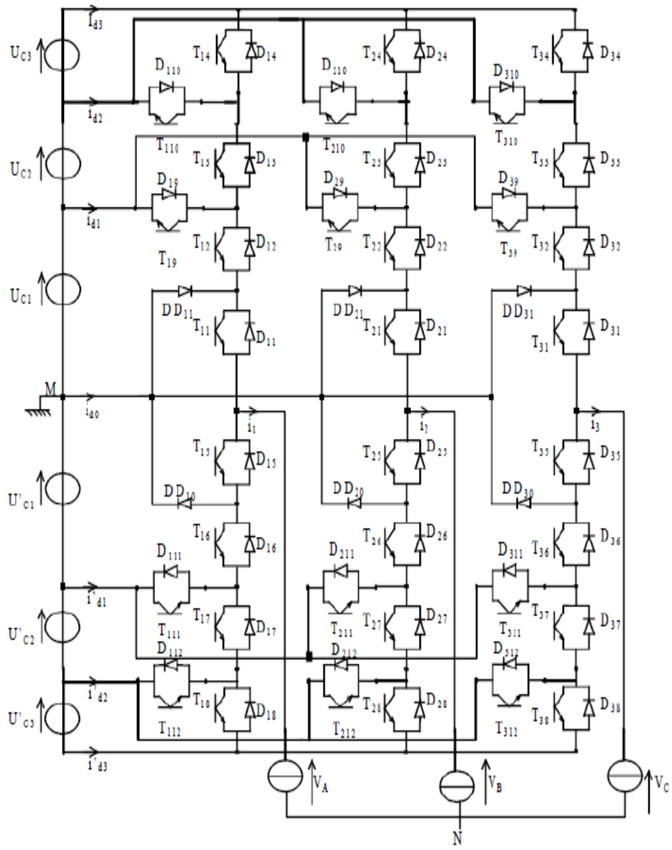

Fig. 1 Seven-level NPC inverter.

4. NSVPWM technique

A very popular strategy with high switching frequency in industrial applications is the space vector modulation (SVM) that uses the principles of space vectors and requires the calculation of sector and angle. In this paper, we propose a new SVPWM technique of seven-level NPC inverter based on calculation of minimum and maximum of voltages. However, this technique is detailed in [7, 8]. The advantage of the proposed seven-level SVPWM strategy that it does not need to calculate the angle and sector, good utlization of DC-link voltage, low current ripple, is simple to implement compared to the traditional SVM technique. The SVPWM technique block represents the seven-level inverter model as shown in Fig. 2.

In order to improve the seven-level SVPWM performances, a additional use of the neural networks (NNs) is proposed. The principle of neural space vector pulse width modulation (NSVPWM) is similar to seven-level SVPWM technique. The difference is the use NNs controllers to replace the hysteresis comparators. As shown in Fig. 3. The seven-level NSVPWM technique gives more minimum of THD value, minimize power ripples, easy to implement and simple scheme compared to traditional SVPWM technique [9].

Table 1. Parameters of the LM algorithm

Parameters of the LM	Values
Number of hidden layer	8
TrainParam.Lr	0.005
TrainParam.show	50
TrainParam.eposh	1000
Coeff of acceleration of convergence (mc)	0.9
TrainParam.goal	0
TrainParam.mu	0.9
Functions of activation	Tensing, Purling, gensim

The main advantage of the NN controller it is that is easy to implement the command and that it has the capability of generalization [10]. The block diagram of NNs controllers based hysteresis comparators is shown in Fig. 26 (see Appendix). The structure of Layer 1 and layer 2 is shown in Fig. 27 and Fig. 28 respectively (see Appendix).

A summary of the convergence of the network obtained by using the value of the parameters is depicted in Table 1.

4. DVC control with seven-level NSPWM technique

The principale is to orient the stator flux along the axis of the rotating frame [11].

$$\psi_{ds} = \psi_s \quad \text{and} \quad \psi_{qs} = 0 \tag{6}$$

On the other hand, by neglecting *Rs* the stator voltage can be expressed by [12, 13]:

$$\begin{cases} V_{ds} = 0 \\ V_{qs} = \omega_s \psi_s \end{cases} \tag{7}$$

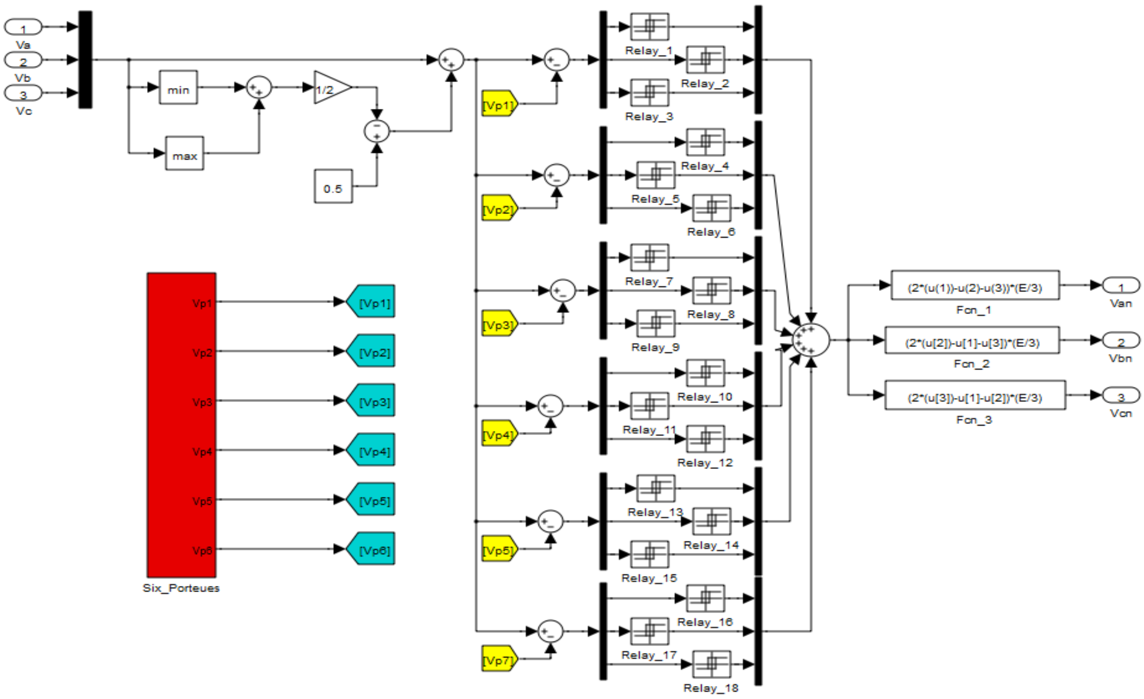

Fig. 2 Seven-level SVPWM technique.

And :

$$\begin{cases} I_{ds} = -\dfrac{M}{L_s} I_{dr} + \dfrac{\psi_s}{L_s} \\ I_{qs} = -\dfrac{M}{L_s} I_{qr} \end{cases} \tag{8}$$

The reactive and active powers consequently given by the following expression :

$$\begin{cases} P_s = -\dfrac{3}{2} \dfrac{\omega_s \psi_s M}{L_s} I_{qr} \\ Q_s = -\dfrac{3}{2} \left(\dfrac{\omega_s \psi_s M}{L_s} I_{dr} - \dfrac{\omega_s \psi_s{}^2}{L_s} \right) \end{cases} \tag{9}$$

The equations of Vdr and Vqr become [14]:

$$\begin{cases} V_{dr} = R_r I_{dr} + (L_r - \dfrac{M^2}{L_s}) p I_{dr} - g\, w_s (L_r - \dfrac{M^2}{L_s}) I_{qr} \\ V_{qr} = R_r I_{qr} + (L_r - \dfrac{M^2}{L_s}) p I_{qr} + g\, w_s (L_r - \dfrac{M^2}{L_s}) I_{dr} + g \dfrac{M V_s}{L_s} \end{cases} \tag{10}$$

In steady state, we can write :

$$\begin{cases} V_{dr} = R_r I_{dr} - g\, w_s (L_r - \dfrac{M^2}{L_s}) I_{qr} \\ V_{qr} = R_r I_{qr} + g\, w_s (L_r - \dfrac{M^2}{L_s}) I_{dr} + g \dfrac{M V_s}{L_s} \end{cases} \tag{11}$$

Fig. 4 represents the DVC strategy of DFIG driven by a seven-level NPC inverter using SVPWM technique. This control scheme gives more harmonic distortion (THD) of stator/rotor current, stator flux ripple, torque ripple and reactive/active powers ripples of the DFIG.

The rotor current has the expression :

$$\begin{cases} I_{dr} = (V_{dr} + g\, w_s (L_r - \dfrac{M^2}{L_s}) I_{qr}) \dfrac{1}{R_r + (L_r - \dfrac{M^2}{L_s}) p} \\ I_{qr} = (V_{qr} - g\, w_s (L_r - \dfrac{M^2}{L_s}) I_{qr} - g \dfrac{M V_s}{L_s}) \dfrac{1}{R_r + (L_r - \dfrac{M^2}{L_s}) p} \end{cases} \tag{12}$$

$$T_{em} = -\frac{3}{2} p \frac{M}{L_s} I_{qr} \psi_{ds} \tag{13}$$

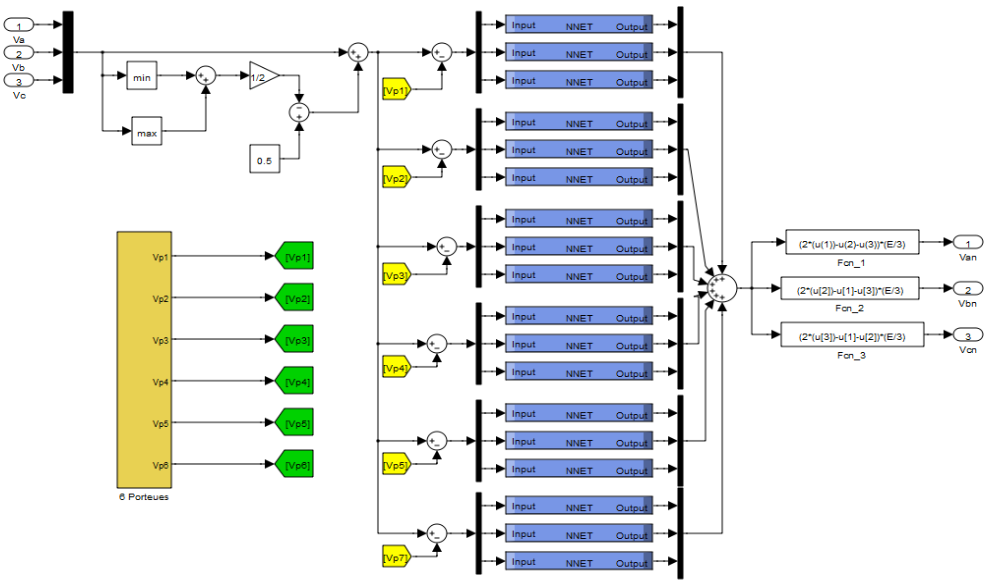

Fig. 3 Seven-level NSVPWM technique.

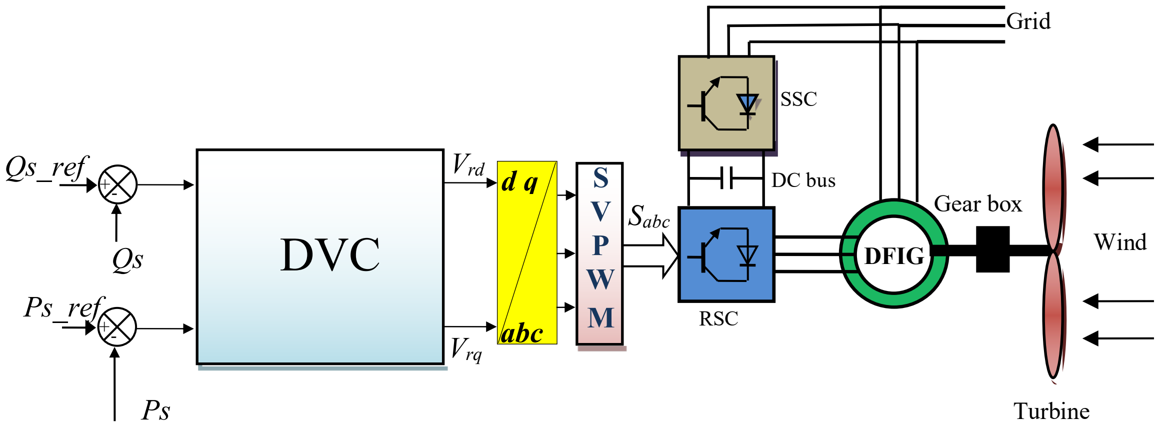

Fig. 4 DVC strategy block with SVPWM technique.

To reduce the harmonic distortion of rotor/stator current, active power ripple, reactive power ripple and torque ripple, we have applied the NSVPWM technique to regulate the active and reactive powers of the DFIG controlled by DVC control scheme. On the other hand, the DVC strategy with seven-level SVPWM strategy is easy to implement and simple scheme.

Fig. 5 represents the DVC strategy of a DFIG driven by a seven-level NSVPWM technique.

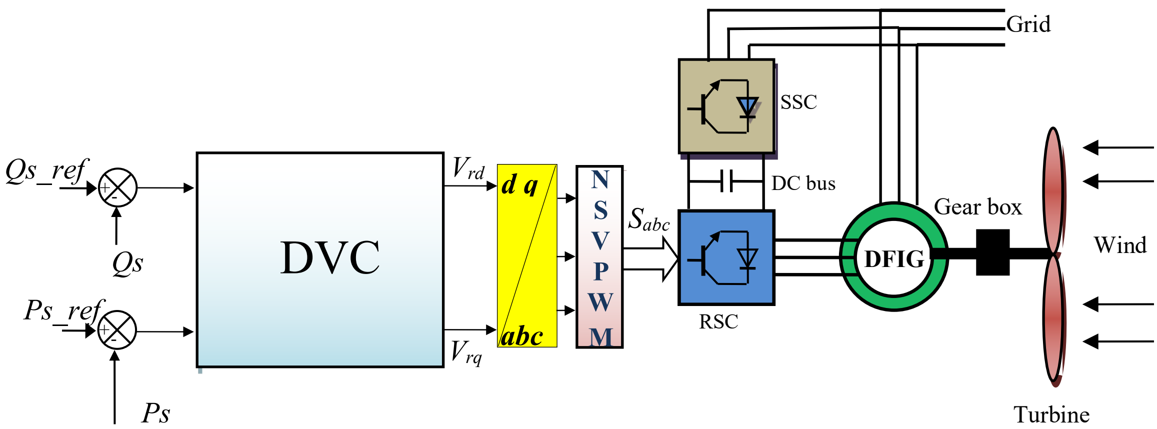

Fig. 5 DVC control with seven-level NSVPWM strategy.

6. Simulation Results

The simulation results of DVC control with seven-level NSVPWM strategy of the 1.5MW DFIG are compared with DVC strategy using seven-level SVPWM technique. For this end, the strategies system was tested under deferent operating conditions such as sudden change of load reactive and active powers. The performance analysis is done with harmonic distortion of stator current, torque, reactive and active powers.

The DFIG used in this case study is a 1.5MW, 380/696V, two poles, 50Hz; with the following parameters: Rr = 0.021Ω, Rs = 0.012Ω, Lr = 0.0136H, Ls = 0.0137H and Lm = 0.0135H. The system has the following mechanical parameters: fr = 0.0024 Nm/s, J = 1000 kg.m2 [16, 17].

A. Reference tracking test (RTT)

From the simulation results presented in Figs. 7-8 it is apparent that the THD value of rotor current for the DVC-7L-NSVPWM is considerably reduced. Table 2 shows the comparative analysis of THD value for rotor current.

Table 2. Comparative analysis of THD value

DVC control with seven-level SVPWM	DVC control with seven-level NSVPWM
1.18%	**0.49%**

For the DVC-7L-NSVPWM and DVC-7L-NSVPWM, the reactive and active powers, tracks almost perfectly their references values (see Figs. 9-10).

Fig. 10 shows the stator current of DVC-7L-SVPWM and DVC-7L-NSVPWM and Fig. 11 shows the electromagnetic torque of DVC-7L-SVPWM and DVC-7L-NSVPWM. From Figs. 12-15 can be seen that the DVC-7L-NSVPWM minimized the torque ripple, stator current ripple, active and reactive powers pulsations compared to DVC-7L-SVPWM control scheme.

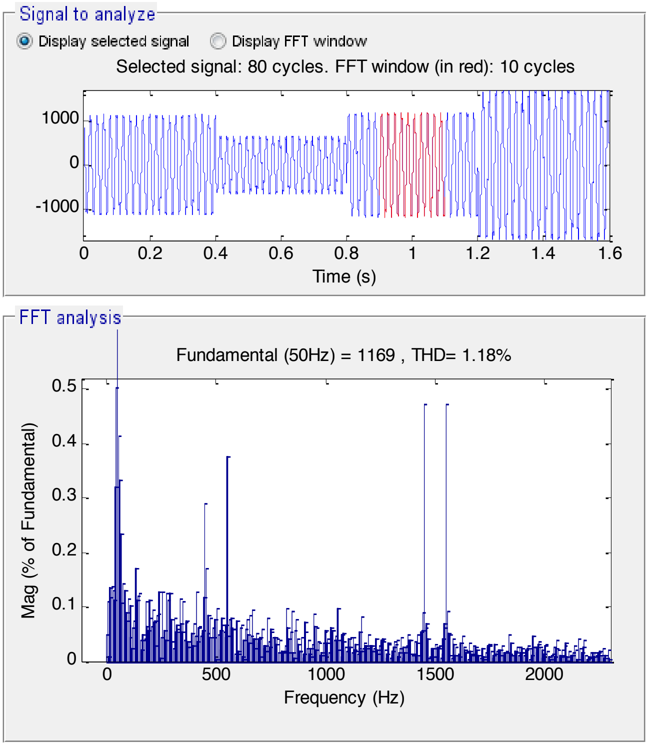

Fig. 6 THD of rotor current for DVC-7L-SVPWM strategy (RTT).

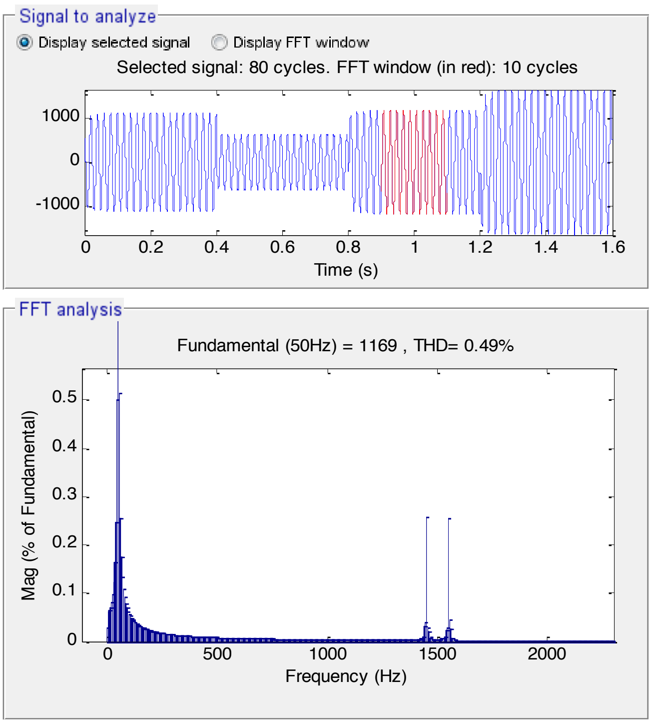

Fig. 7 THD of rotor current for DVC-7L-NSVPWM strategy (RTT).

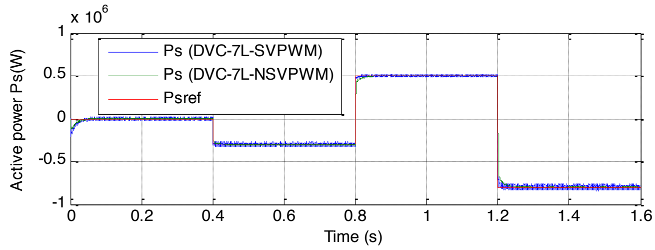

Fig. 8 Active power (RTT).

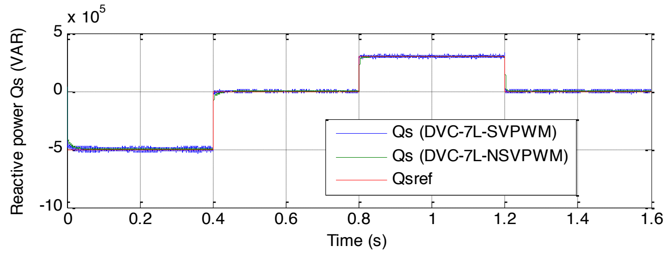

Fig. 9 Active power (RTT).

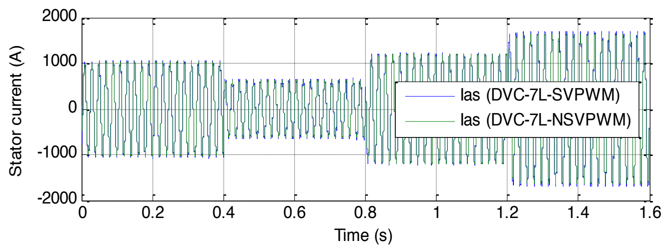

Fig. 10 Stator current (RTT)

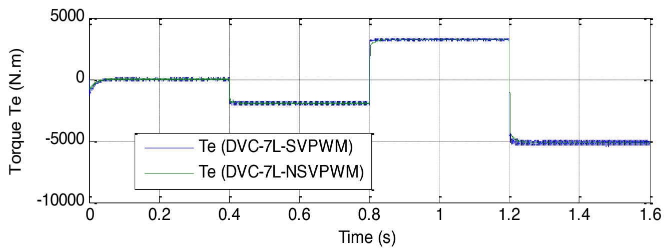

Fig. 11 Torque (RTT).

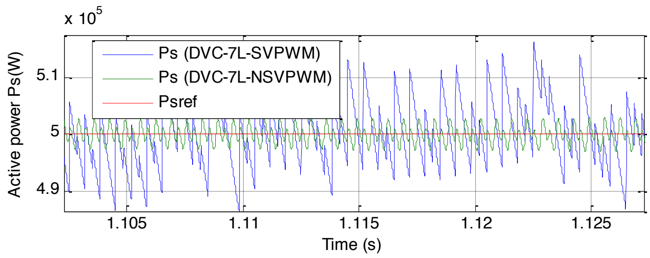

Fig. 12 Zoom in the active power (RTT).

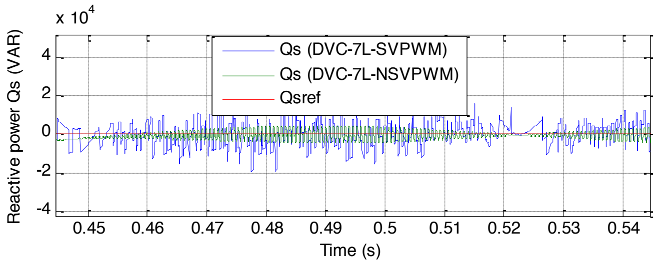

Fig. 13 Zoom in the reactive power (RTT).

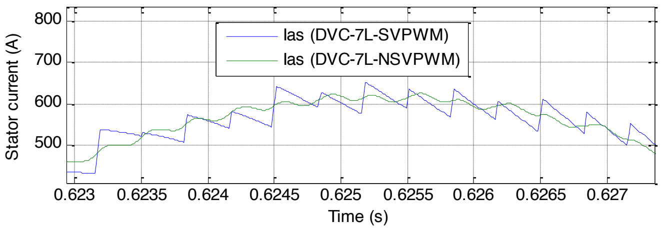

Fig. 14 Zoom in the stator current (RTT).

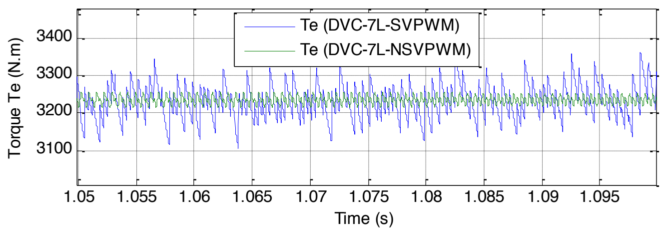

Fig. 15 Zoom in the torque (RTT).

B. Robustness test (RT)

In the following section, the nominal value of the Rr and *Rs* is doubled, the values of inductances *Ls*, M, and Lr are halfed. Simulation results are presented in Figs. 16-17 and Figs. 18-21. As shown, these variations present a clear effect on the active power, reactive power, rotor current and torque. However, the effect appears more important for the DVC-7L-SVPWM control scheme compared to DVC-7L-NSVPWM control (see Figs. 22-25). On the other hand, the THD value of rotor current in the DVC-7L-NSVPWM has been significantly minimized. Table 3 shows the comparative analysis of THD value. Thus it can be concluded that the DVC-7L-NSVPWM control technique is more robust than the DVC-7L-SVPWM control scheme.

Table 3. Comparative Analysis of THD Value (RT)

DVC control with seven-level SVPWM	DVC control with seven-level NSVPWM
4.10%	**1.21%**

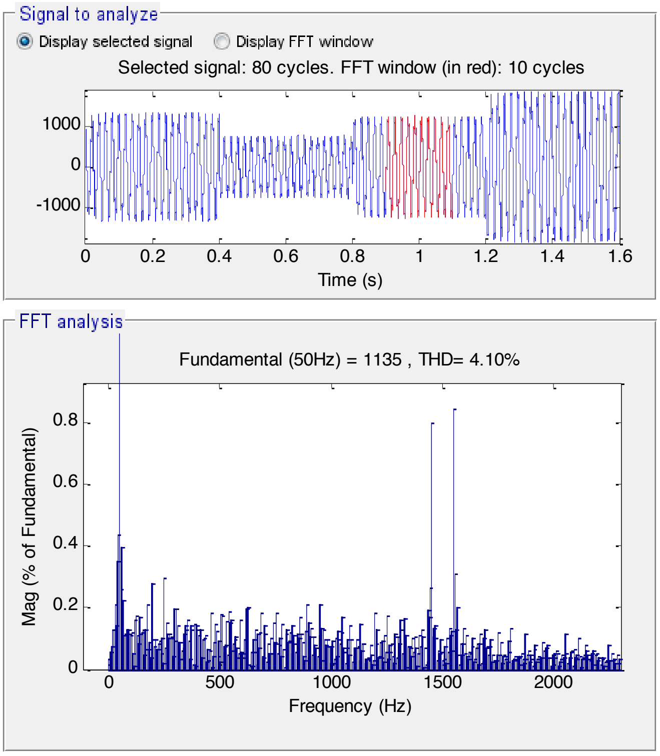

Fig. 16 THD of rotor current for DVC-7L-SVPWM strategy (RT).

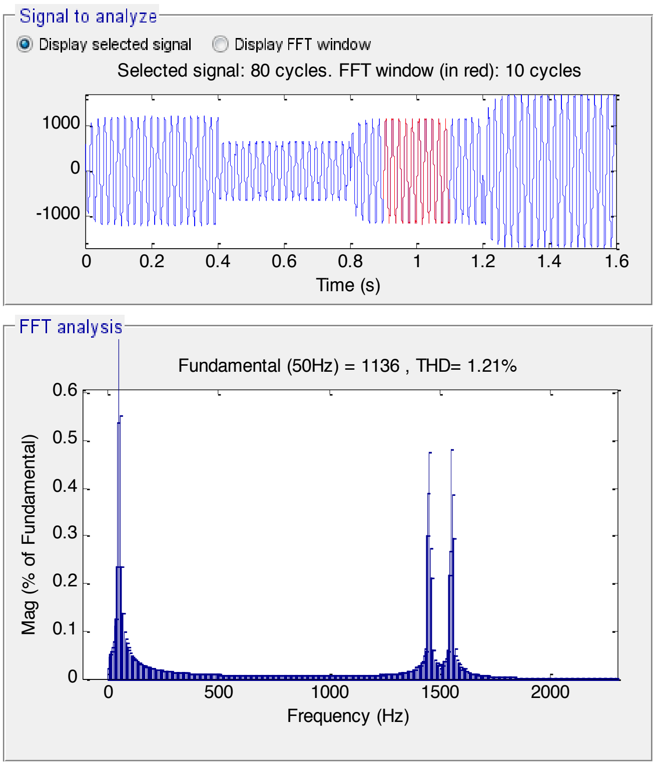

Fig. 17 THD of rotor current for DVC-7L-NSVPWM strategy (RT).

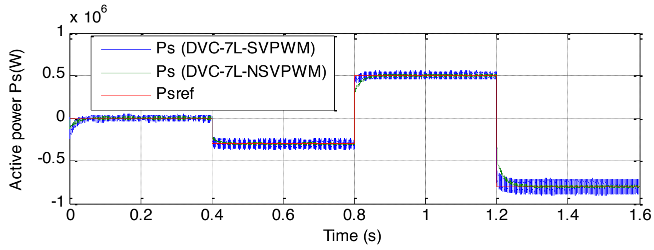

Fig. 18 Active power (RT).

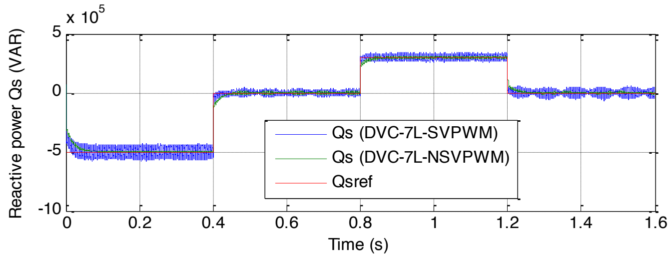

Fig. 19 Reactive power (RT).

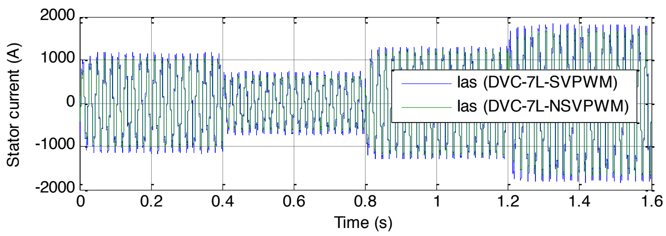

Fig. 20 Stator current

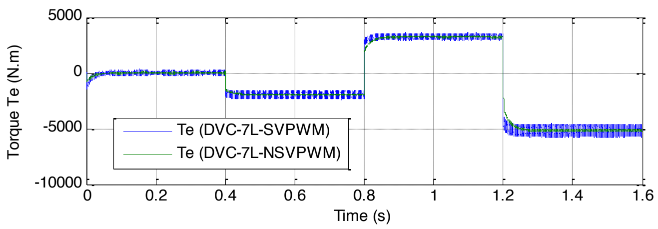

Fig. 21 Torque (RT).

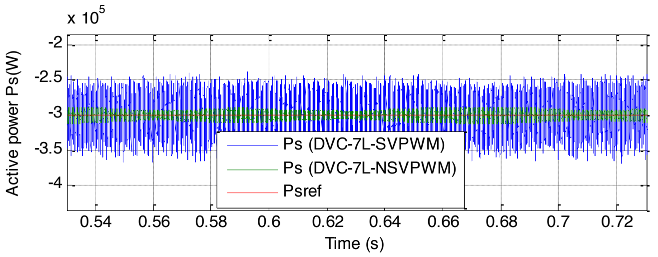

Fig. 22 Zoom in the active power (RT).

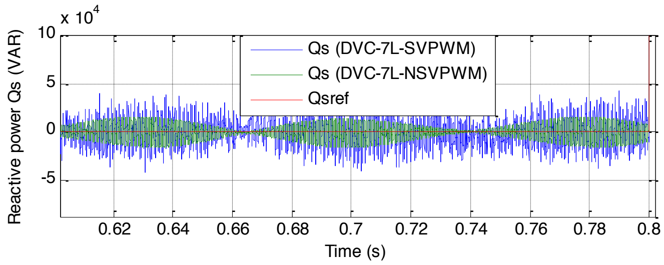

Fig. 23 Zoom in the reactive power (RT).

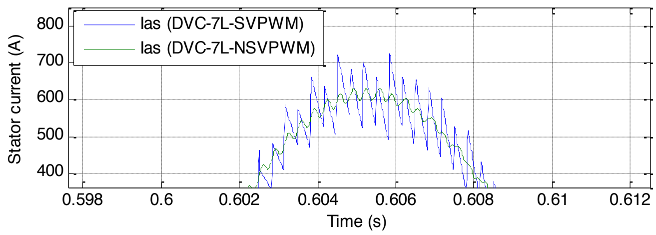

Fig. 24 Zoom in the stator current (RT).

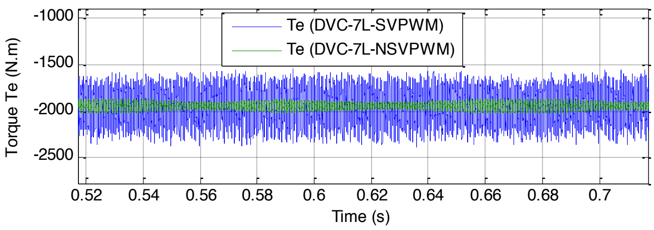

Fig. 25 Zoom in the torque (RT).

7. Conclusions

In this work, the DVC principle is presented and it is shown that with NSVPWM for a seven-level NPC inverter. The simulation results obtained for the DVC control with intelligent SVPWM illustrate a considerable reduction in active power ripple, torque ripple, reactive power ripple and harmonic distortion of rotor current compared to the DVC control scheme utilizing seven-level SVPWM technique.

Appendix

a)ANN controller

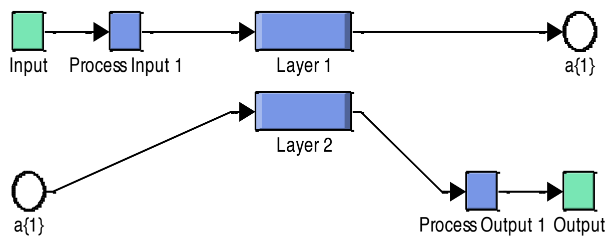

Fig. 26 Block diagram of the ANN controller.

b) Layer 1 and layer 2

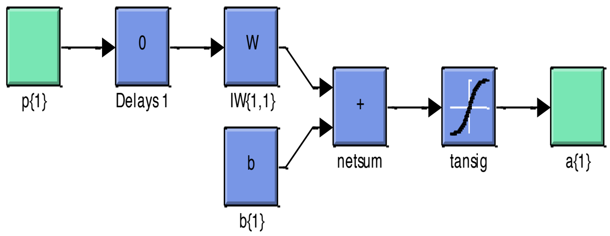

Fig. 27 Layer 1.

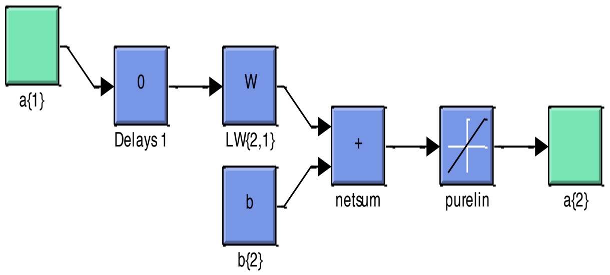

Fig. 28 Layer 2.

Reference

[1] H. Benbouhenni, « Neuro-sconde order sliding mode field oriented control for DFIG based wind turbine, » International Journal Of Smart Grid, Vol. 2, No. 4, pp. 209-217, 2018.
[2] H. Benbouhenni, « Comparative Study between direct vector control and fuzzy sliding mode controller in three-level space vector modulation inverter of reactive and active power command of DFIG-based wind turbine systems, » International Journal Of Smart Grid, Vol. 2, No. 4, pp. 188-196, 2018.
[3] F. Chabni, R. Taleb, M. Helaimi, « ANN-based SHEPWM using a harmony search on a new multilevel inverter topology, » Turkish Journal of Electrical Engineering & Computer Sciences, Vol. 25, pp. 4867-4879, 2017.
[4] H. Benbouhenni, R. Taleb, « Etude comparative entre la DTC neuronale à sept niveaux et la DTC neuronale à cinq niveaux de la machine asynchrone, » 1st Algerian Multi-Conference on Computer, Electrical and Electronic Engineering (AMCEE'17), 24-27 April 2017, Algiers, Algeria.
[5] S. Ramahlingam, A. Benjamin, T. Sutikno, L. Logan Raj, «Improvise 3-level DTC of induction machine using constant switching frequency method by utilizing multiband carrier, » International Journal of Power Electronics and Drive System, Vol. 7, No. 3, pp. 638-647, 2016.
[6] H. Benbouhenni, «Seven-level direct torque control of induction motor based on artificial neural networks with regulation speed using fuzzy PI controller, » Iranian Journal of Electrical and Electronic Engineering, Vol. 14, No.1, pp. 85-94, 2018.
[7] H. Benbouhenni, Z. Boudjema, A. Belaidi, « Using three-level Fuzzy space vector modulation method to improve indirect vector control strategy of a DFIG based wind energy conversion systems, » International Journal Of Smart Grid, Vol. 2, No.3, pp.155-171, 2018.
[8] H. Benbouhenni, Z. Boudjema, A. Belaidi, « Indirect vector control of a DFIG supplied by a two-level FSVM inverter for wind turbine system, » Majlesi Journal of Electrical Engineering, Vol. 13, No. 1, pp. 45-54, 2019.
[9] H. Benbouhenni, «Direct power control of a DFIG fed by a seven-level inverter using SVM strategy, » International Journal Of Smart Grid, Vol. 3, No. 2, pp. 54-62, 2019.
[10] H. Benbouhenni, Z. Boudjema, A. Belaidi, « Neuro-second order sliding mode control of a DFIG supplied by a two-level NSVM inverter for wind turbine system, » Iranian Journal of Electrical and Electronic Engineering, Vol.14, No. 3, pp. 362-373, 2018.
[11] H. Benbouhenni, Z. Boudjema, A. Belaidi, « Direct vector control of a DFIG supplied by an intelligent SVM inverter for wind turbine system, » Iranian Journal of Electrical and Electronic Engineering, Vol.15, No. 1, pp. 45-55, 2019.
[12] H. Benbouhenni, Z. Boudjema, A. Belaidi, « DFIG-based wind turbine system using three-level neural space vector modulation technique, » Majlesi Journal of Mechatronic Systems, Vol. 7, No. 2, pp. 35-45, 2018.
[13] H. Benbouhenni, « Comparative study between different vector control methods applied to DFIG wind turbines, » Majlesi Journal of Mechatronic Systems, Vol. 7, No. 4, pp. 15-23, 2018.
[14] H. Benbouhenni, « Comparative Study between Direct Vector Control and Fuzzy Sliding Mode Controller in Three-Level Space Vector Modulation Inverter of Reactive and Active Power Command of DFIG-Based Wind Turbine Systems, » International Journal Of Smart Grid, Vol. 2, No. 4, pp. 188-196, 2018.
[15] H. Benbouhenni, «Direct vector control for doubly fed induction generator-based wind turbine system using five-level NSVM and two-level NSVM technique, » International Journal Of Smart Grid, Vol. 3, No. 1, pp. 25-32, 2019.
[16] H. Benbouhenni, Z. Boudjema, A. Belaidi, « Using four-level NSVM technique to improve DVC control of a DFIG based wind turbine systems, » Periodica Polytechnica Electrical Engineering and Computer Science, Vol. 63, No. 3, 2019.
[17] H. Benbouhenni, « A comparative study between FSMC and FSOSMC strategy for a DFIG-based wind turbine system,» Majlesi Journal of Mechatronic Systems, Vol. 8, No. 2, 2019.